Int J Adv Manuf Technol (2017) 92:989–999
DOI 10.1007/s00170-017-0202-8

ORIGINAL ARTICLE

Automatic recognition system of welding seam type based on SVM method

Junfeng Fan[1,2] · Fengshui Jing[1,2] · Zaojun Fang[1] · Min Tan[1,2]

Received: 4 October 2016 / Accepted: 22 February 2017 / Published online: 7 March 2017

Abstract In this paper, an automatic recognition system of welding seam type based on support vector machine (SVM) method is presented. The hardware of the proposed system consists of an industry robot with six degrees of freedom, a vision sensor, and a computer. The system has two parts including input feature vector computation and model building. In the input feature vector computation part, the depth values of a series of points of the welding joint are taken as feature vector, which are determined by four steps including main line extraction of the laser stripe, normalization of the laser stripe, selection of the left and right edge points of the welding joint, and normalization of feature vectors. In the model building part, SVM-based modeling method is used to achieve welding seam type recognition. At first, RBF kernel function is employed for classification of welding seam types. Then, the parameters of RBF are determined by a grid search method using cross-validation. After the optimal parameters of RBF being determined, the SVM model is built, and it could be used to predict welding seam type. Finally, a series of welding seam type recognition experiments are implemented. Experimental results show that the proposed system can achieve welding seam type recognition accurately and the computation cost can be reduced compared with previous methods.

Keywords Welding seam type recognition · Structured-light vision · SVM method · Feature extraction

✉ Fengshui Jing
fengshui.jing@ia.ac.cn

Junfeng Fan
fanjunfeng2014@ia.ac.cn

Zaojun Fang
zaojun.fang@ia.ac.cn

Min Tan
tan@compsys.ia.ac.cn

[1] The State Key Laboratory of Management and Control for Complex Systems, Institute of Automation, Chinese Academy of Sciences, Beijing 100190, China

[2] University of Chinese Academy of Sciences, Beijing 100049, China

1 Introduction

At present, more and more industrial robots have been widely applied in welding processes. However, most of them used in factory belong to the teach-and-playback robots. These robots have some fatal weakness. At first, they require a lot of time to be taught in advance that leads to low working efficiency. In addition, they cannot self-rectify deviations during the welding process. That means any deviation of the weld joint from the ideal condition may cause poor weld quality. What is more, the seam position is often disturbed by distortion, ways of spreading heat, and variability of gap, so the quality of welding forming will be affected.

In order to solve these problems, many seam tracking systems have been used in welding processes. One distinct feature of automated seam tracking systems is that they can sense the seam information by some kinds of sensors. In the last decades, many different sensors have been developed and used in welding robots including acoustic sensors [1], inductive sensors [2], ultrasonic sensors [3], and arc sensors [4]. Recently, vision sensors have gotten more and more attention due to their features of non-contact, high-precision and huge information [5–17]. Among them, structured-light

vision sensors are widely used in welding process due to the monochromaticity and robustness of the laser light. Many seam tracking systems have been designed with structured-light vision sensors. In the welding production, according to the groove form and the different ways of connection, welding seam types are the following: symmetric V groove, left and right side V groove, I groove, and left and right lap joint groove [19]. Structured-light stripe images of the different welding seam types are different from each other. Thus, specific image features extraction algorithm is developed according to the welding seam type. At the same time, in the robot welding, the welding speed, voltage, current and other parameters need to be adjusted according to the welding seam type. However, most of the developed vision systems need to enter the welding seam type manually before welding. Thus, it seriously reduced the adaptability and automation level of the welding robot. In recent years, some researchers have carried out some researches on the automatic recognition of welding type. Qian *et al*. [18] proposed an automatic recognition method of welding seam type based on structured-light. This method achieves welding seam type recognition using two steps. In the first step, the location of laser stripe was searched. In the second step, welding seam type recognition was achieved. However, this method achieves the recognition of welding seam type based on lots of determination of relative relationship of the coordinate values of these feature points. So this method is more complex. Li *et al*. [19] presented a method to identify the welding seam type based on the Hausdorff distance. This method matches laser stripe pattern with the entire templates in the reference model library, so the computation cost is huge and it will affect real-time performance. Therefore, it is urgent to develop a high accurate and fast welding seam type recognition algorithm, which is the premise of welding automation.

As an intelligent machine learning method, support vector machine (SVM) method has gotten more and more attention because it not only has a rigorous theoretical background but also can find global optimal solutions. This method is especially suitable for problems with small training samples, high dimension and non-linearity [20, 21].

In this paper, a welding seam type recognition system is designed based on SVM method, which has three distinguish characteristics. Firstly, most of noises from arc lights and splashes can be filtered out by using a narrow band optical filter and ”min operation”, that is the prerequisite for welding seam type recognition. Secondly, SVM-based modeling method is used to utilize input feature vectors to build a model that achieve welding seam type recognition accurately. Thirdly, the computation cost of welding seam type recognition based on the proposed methods in this paper can be reduced compared with previous methods. Therefore, during the welding process of a number of different welding seam types of workpieces, the welding seam type of each workpiece can be determined accurately and fast before welding using the proposed system. Thus, the corresponding image feature point extraction algorithm of this welding seam type can be automatically selected to achieve seam tracking of this work-piece in the following welding process.

The rest of the paper is organized as follows. Section 2 describes the system configuration. The input feature vector computation is discussed in detail in Section 3. The SVM model building is presented in Section 4. In Section 5, the experiments and results are provided to verify the performance of the proposed recognition system of welding seam type. Finally, the paper is concluded in Section 6.

2 System configuration

2.1 Hardware of recognition system

As shown in Fig. 1, the recognition system is composed of three parts: the robotic system, the vision sensor, and the computer. The robotic system is an industry robot with six degrees of freedom made by YASKAWA Corporation. The vision sensor device is composed of a charge-coupled device (CCD) camera, a stripe laser, and an optical filter. The camera is mounted ahead of the welding torch by a fixed distance. Its viewing direction is the same as that of the torch. The laser emitter forms a laser plane in the front of the camera. It intersects with the workpiece and forms a structured laser stripe. A narrow band optical filter is placed in front of the focus lens. The computer, which is an industrial computer, runs the image processing, welding seam type recognition algorithm, and acts as the interface for this system.

2.2 Vision sensor system design

Vision sensor system is an important part of the welding seam type recognition system. It will directly affect the accuracy of welding seam type recognition. If the image acquired by vision sensor is not perfect, it will make the welding seam type recognition very difficult. In this paper, the design of laser vision sensor is shown in Fig. 2, which is composed of a CCD camera, a stripe laser, and a filter. The CCD camera is the most important component because it has direct and significant influence on the quality of image acquisition. A HV-1351UM-M industrial camera with a 16-mm focal length is used. In addition, a 635-nm stripe laser and a narrow band optical filter with pass band centered at

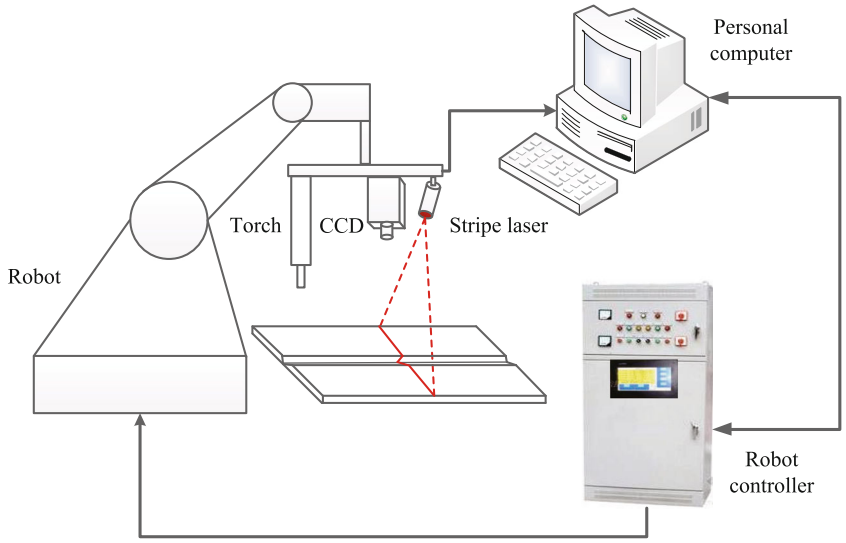

Fig. 1 The schematic diagram of the recognition system

635 nm are adopted. In this way, most of the noises from arc lights would be filtered out.

3 Input feature vector computation

3.1 Welding seam type classification

In the welding production, according to the groove form and the different ways of connection, welding seam types are the following: symmetric V groove, left and right side V groove, I groove, and the left and right lap joint groove. The structured-light images of different welding seam types during welding are as shown in Fig. 3.

It is shown that the laser stripe is composed of a series of piecewise linear segments. The laser stripe is generally straight on both sides of the surface of the work piece, and the specific shape is formed in the welding joints, such as groove deformation or step jump.

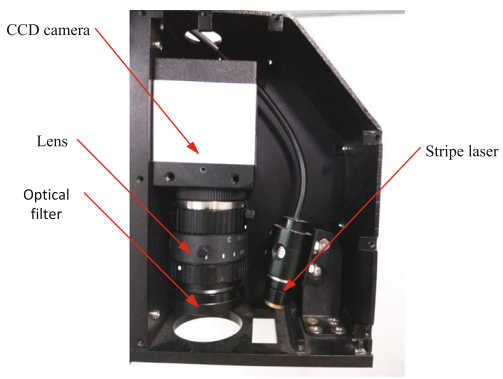

Fig. 2 The laser vision sensor

3.2 Laser stripe extraction

In order to determine the input feature vector of the classification model, center profile of the laser stripe needs to be extracted firstly, because the shapes of laser stripes formed by different welding seam types are different. In the following sections, three steps are designed to extract the center profile of the laser stripe: (1) image pre-processing, (2) ROI computation, and (3) center line extraction.

3.2.1 Image pre-processing

Although the welding seam type needs to be determined before welding, the structured-light images could be polluted by the ambient arc lights and splashes, because there may be two more welding robots working together in the same workshop. Since most of noises from arc lights would be filtered out by using a narrow band optical filter as shown in Fig. 3, the purpose of the image pre-processing is to eliminate the influence of the splashes. Due to the instantaneity of the splashes, most of splashes last for less than one sample period, while the laser stripe in the image is stable. Based on this fact,the influence of these disturbances can be removed by the following "min operation" between the last image and current image [13, 17]:

$$I(i, j, t) = \min[I(i, j, t-1), I(i, j, t)], \quad (1)$$

where $I(i, j, t)$ is the gray value of the pixel (i, j) in current time t, and i and j are the rows and columns of the image. Meanwhile, there exist some other noises due to the non-uniformity of surface. The median filter is used to eliminate them. After the image pre-processing, most of the noises can be removed.

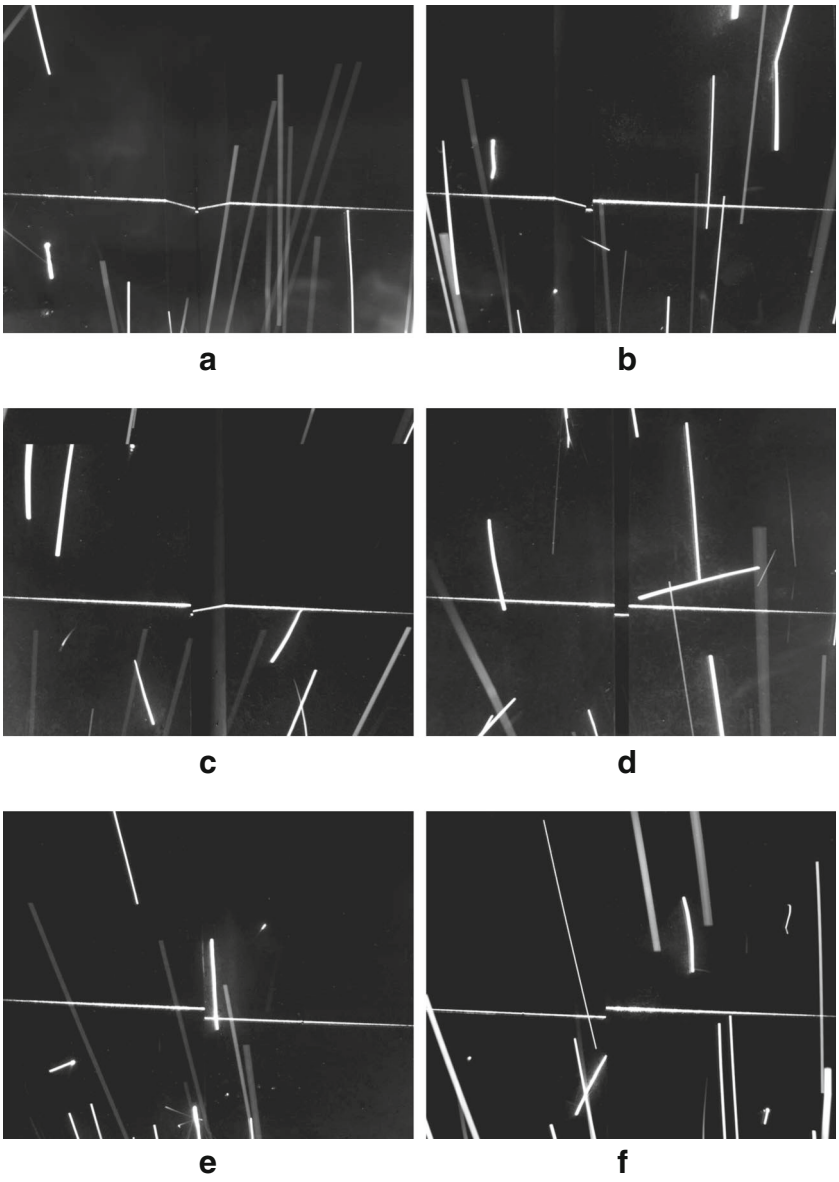

Fig. 3 The structured-light images of different welding seam types during welding. **a** The structured-light image of symmetric V groove. **b** The structured-light image of left V groove. **c** The structured-light image of right V groove. **d** The structured-light image of I groove. **e** The structured-light image of left lap groove. **f** The structured-light image of right lap groove

3.2.2 ROI computation

During the image processing, an image with large size generally not only brings expensive computational burden to the image processing but also sacrifices the real-time performance. In order to reduce the computational cost in image processing and improve the real-time performance, the ROI is used in this paper. Since the laser stripe is approximately parallel with the u axis of the image, the ROI can be determined by projecting the gray value onto v axis. The projection operation is carried out every row with Eq. 2, and the projection result is shown in Fig. 4.

$$J_v(i) = \sum_{j=1}^{w} I(i, j) \quad (i = 1, 2, \cdots, h), \tag{2}$$

where $J_v(i)$ is the projection value of i-th row of pixels on v axis, and w and h are the width and height of the image respectively.

The ROI of the laser stripe in the image is computed with Eq. 3:

$$\begin{cases} [x_{\text{lmin}}, x_{\text{lmax}}] = [1, w] \\ [y_{\text{lmin}}, y_{\text{lmax}}] = [v_c - \Delta y, v_c + \Delta y], \end{cases} \tag{3}$$

where $[x_{\text{lmin}}, x_{\text{lmax}}]$ and $[y_{\text{lmin}}, y_{\text{lmax}}]$ are the x-range and y-range of the ROI of the laser stripe, Δy is the threshold value for computing the y-range, and v_c is the row index with the greatest projection value.

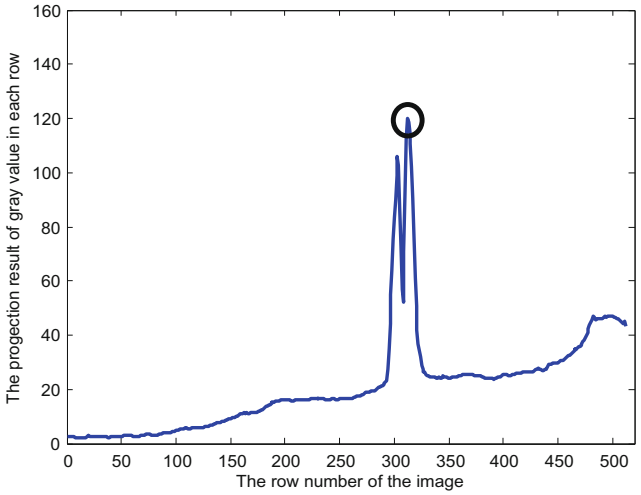

Fig. 4 The projection result of gray value in each row

3.2.3 Center profile extraction

In order to extract the center profile of the laser stripe, the upper border and lower border of the laser stripe should be detected firstly. The upper border and lower border of laser stripe is detected by computing the greatest and least gradient gray value in each column as follows [22]:

$$P_{lu}(j) = arg\max_{k} G(k) \qquad (j = 1, 2, \cdots, w) \tag{4}$$

$$P_{ll}(j) = arg\min_{k} G(k) \qquad (j = 1, 2, \cdots, w) \tag{5}$$

$$G(k) = \sum_{i=k}^{k+2} \alpha_{i-k+1} I(i, j) - \sum_{i=k-3}^{k-1} \alpha_{i-k+4} I(i, j), \tag{6}$$

where $P_{lu}(j)$ is the upper border point in j-th column, $P_{ll}(j)$ is the lower border point in j-th column, $G(k)$ is the gradient gray value in k-th point of j-th column, $I(i, j)$ is the gray value of pixel point (i, j), w is the width of the ROI of image, and $\alpha_i (i = 1, 2, 3)$ are the coefficients of the gradient operator. Then, the center profile of laser stripe is computed using Eq. 4:

$$P_{lc}(j) = (P_{lu}(j) + P_{ll}(j))/2 \qquad (j = 1, 2, \cdots, w). \tag{7}$$

The center profile extraction results of laser stripes of different welding seam types are as shown is Fig. 5.

3.3 Input feature vector computation

From the above methods, the center profile of the laser stripe is extracted. Then, the input feature vectors are determined by four steps including main line extraction of the laser stripe, normalization of the laser stripe, selection of the left and right edge points of the welding joint, and normalization of feature vectors.

3.3.1 Main line extraction of the laser stripe

After the center profile of laser stripe is computed by previous methods, Hough transform is applied to extract the main line of the laser stripe. The angle from the v axis to a line is represented with θ. The distance from the origin of image coordinates to the line is defined as ρ. Thus, the line parameters are expressed as (ρ, θ) in the polar coordinates. The resolution of parameter θ is set to 0.5°. Since the laser stripe is approximately parallel with the u axis of the image, the range of θ is set as [70, 110] in the polar coordinates. If the distance from a point on the center profile to the main line obtained by Hough transform is less than a preset threshold d_T, it is accepted as an inner point. Then, least square fitting technique is applied to these inner points to compute the accurate main line of the laser stripe. Suppose the main line of the laser stripe is

$$y = kx + b, \tag{8}$$

where k and b are the slope and intercept of the laser stripe respectively. The least square line fitting equation is expressed with Eq. 9:

$$\begin{cases} \widetilde{k}_l = \dfrac{\sum_{i=1}^{n} x_i y_i - n\overline{x}\,\overline{y}}{\sum_{i=1}^{n} x_i^2 - n\overline{x}^2} \\ \widetilde{b}_l = \overline{y} - \widetilde{k}_l \overline{x} \end{cases}, \tag{9}$$

where $\widetilde{k}_l$ and $\widetilde{b}_l$ are the parameters of fitted laser stripe, $(x_i, y_i)(i = 1, 2, \cdots, n)$ are the inner points, n is their number, and $(\overline{x}, \overline{y})$ are the average coordinates of the inner points.

3.3.2 Normalization of the laser stripe

According to the angle from the u axis to the extracted main line, the rotation transformation is carried out the center profile of laser stripe and the main line is transformed into the direction paralleling to the u axis using Eq. 10:

$$L_h(i) = \begin{bmatrix} \cos\theta & -\sin\theta \\ \sin\theta & \cos\theta \end{bmatrix} m_h(i), \tag{10}$$

where $m_h(i)$ is coordinates of the i-th point on the center profile of laser stripe and $L_h(i)$ is coordinates of the i-th point the center profile of laser stripe after normalization

3.3.3 Selection of the left and right edge points of the welding joint

Due to rich information of the deformation part of the laser stripe, which is produced at the welding joint, we only focus

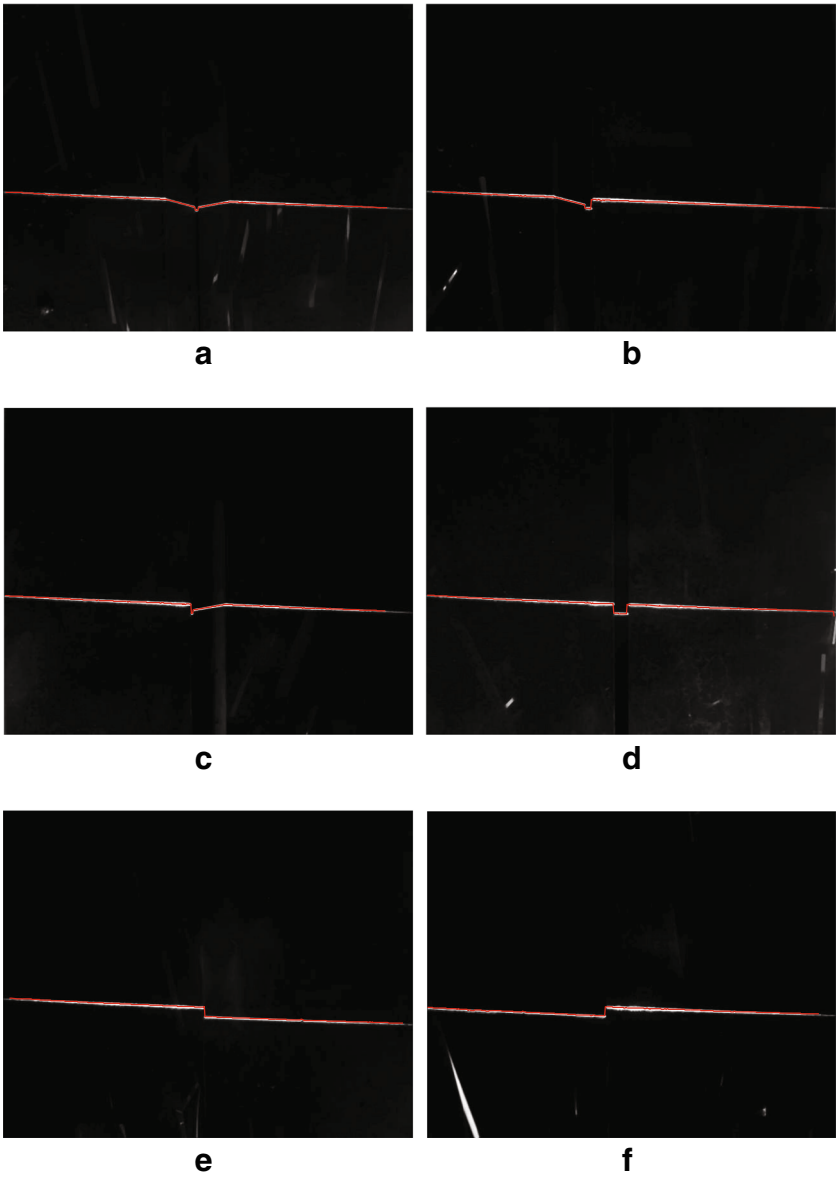

Fig. 5 The laser stripe extraction images of the different welding seam types. **a** The laser stripe extraction image of symmetric V groove. **b** The laser stripe extraction image of left V groove. **c** The laser stripe extraction image of right V groove. **d** The laser stripe extraction image of I groove. **e** The laser stripe extraction image of left lap joint. **f** The laser stripe extraction image of right lap joint

on the laser stripe at the welding joint. Thus, the left and right edge points of the welding joint are determined firstly. Searching for points on the center profile of laser stripe from left to right, when all the distances from some continuous points on the center profile of laser stripe to the main line are more than a preset threshold d_t, the first point among these continuous points is regarded as the left edge point of the welding joint. In the same way, searching for points on the center profile of laser stripe from right to left, the right edge point of the welding joint can be determined.

3.3.4 Normalization of feature vectors

After the left and right edge points of the welding joint are determined by previous methods, feature vectors can be determined as follows. As shown in Fig. 6, suppose the left edge point of the welding joint is P_i, and right edge point of the welding joint is P_j. P_i and P_j are the i-th point and j-th point on the center profile of laser stripe. Then, nine feature points can be determined using Eq. 11:

$$\begin{cases} l = \lfloor i + \frac{j-i}{8}(k-1) \rfloor \\ FP_k = P_l \, (k = 1, 2, \cdots, 9) \, , \end{cases} \tag{11}$$

where P_l is l-th point on the center profile of laser stripe and FP_k is the k-th feature point. Then, the distances h_k $(k = 1, 2 \cdots 9)$ between these points and the main line of the laser stripe are calculated, respectively. Finally, the normalization is used to decrease the influence of large value data, which is computed using Eq. 12:

$$\overline{h}_k = \frac{h_k}{\max\{h_k\}} \, (k = 1, 2, \cdots, 9) \, . \tag{12}$$

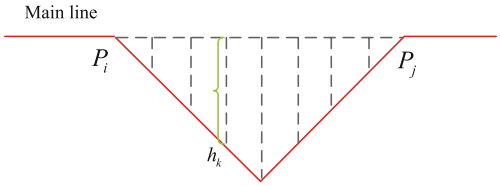

Fig. 6 Input feature vector computation method

Then, the feature vector is expressed as $\left[\overline{h}_1, \overline{h}_2, \cdots, \overline{h}_9\right]^T$.

To verify the effectiveness of the proposed input feature vector computation method, many structured-light images of different welding seam types have been tested. Since the processing procedure is the same for six different welding seam types, so we take symmetric V groove as example. The processing procedure and feature vector extraction result for one image is shown in Fig. 7. It is seen that the image feature vector can be accurately extracted by using the proposed image processing method.

4 SVM model building

4.1 Procedure of SVM-based modeling method

The whole procedure of SVM modeling method is shown in Fig. 8. At first, the structured-light image is captured by the CCD camera. Second, the obtained image is processed and input feature vectors are determined. Third, the input feature vectors are used to build SVM model by deciding kernel function and optimizing its parameters. When the SVM model meets the accuracy requirements of welding seam type identification, it is used to predict the sampling data online. The input feature vectors have been determined using the above method. Then, the SVM model building is described in detail.

4.2 SVM modeling

As shown in Fig. 9, SVM is a binary classifier, and it tries to find an optimal hyper-plane $w^T\phi(x) + b = 0$ that maximizes the margin between the feature vectors of all samples data in two classes. Essentially, the building of SVM model is to obtain an optimal hyper-plane. One way of obtaining this is by solving the optimization problem with Eq. 13:

$$\begin{cases} \min\limits_{w,b} \frac{1}{2}\|w\|^2 \\ s.t.\ y_i\left(w^T x_i + b\right) \geq 1, (i = 1, 2, \cdots, m)\,. \end{cases} \tag{13}$$

The assumption here is that there exists a function $f(x) = w^T x + b$ that makes all samples correctly classified. However, this may lead to over fitting. In order to overcome

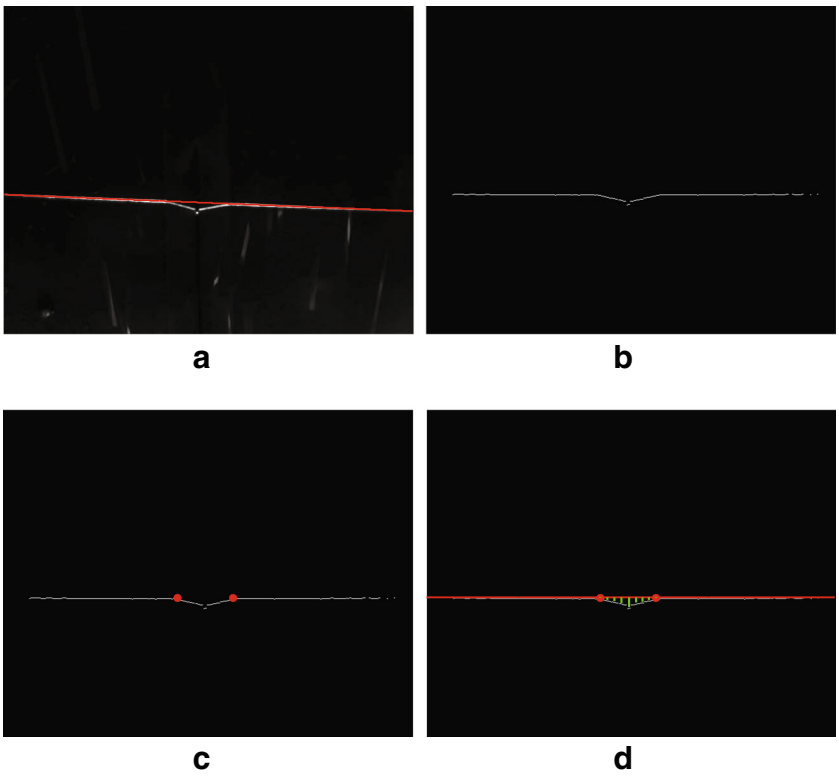

Fig. 7 The procedure of the feature vector computation of a structured-light image. **a** Main line extraction of the laser stripe. **b** Normalization of the laser stripe. **c** Selection of the left and right edge points of the weld joint. **d** Normalization of feature parameters

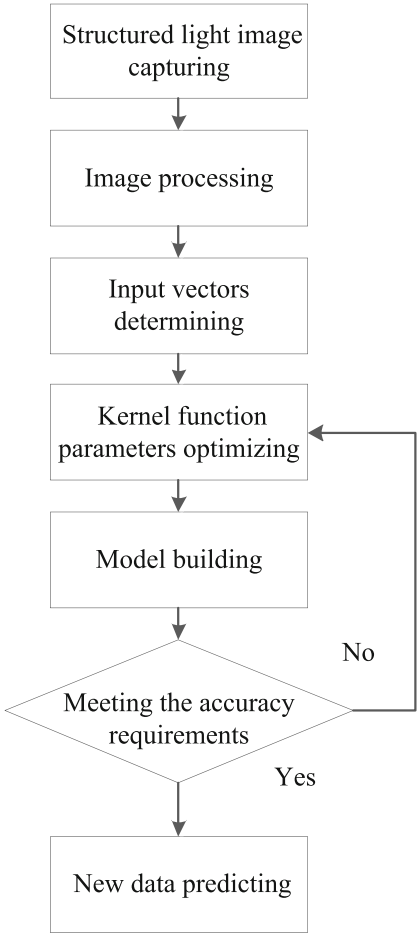

Fig. 8 Procedure of the SVM modeling method

this problem, the slack variables ξ_i are introduced. The formulation can be restated with Eq. 14:

$$\begin{cases} \min\limits_{w,b,\xi_i} \frac{1}{2}\|w\|^2 + C\sum_{i=1}^{m}\xi_i \\ s.t.\ y_i\left(w^T x_i + b\right) \geq 1 - \xi_i \\ \quad \xi_i \geq 0, (i = 1, 2, \cdots, m), \end{cases} \tag{14}$$

where C is a regularization parameter and controls the trade-off between maximizing the margin and minimizing the training error. Too small C leads to under fitting and too large C leads to over fitting. To make the training process stable, C should be set large enough [23]. In the previous discussion, the training samples are considered to be linearly separable. However, there may not be a hyper-plane that can classify all the samples correctly. In order to solve this problem, SVM maps the training patterns from the input space X to a high-dimensional feature space F, which makes samples linearly separable in the feature space. This is represented with Eq. 15:

$$f(x) = w^T\phi(x) + b, \tag{15}$$

where $\phi : X \rightarrow F$: is a nonlinear map from the input space to the feature space. The optimization formulation can be restated with Eq. 16:

$$\begin{cases} \min\limits_{w,b,\xi_i} \frac{1}{2}\|w\|^2 + C\sum_{i=1}^{m}\xi_i \\ s.t.\ y_i\left(w^T\phi(x_i) + b\right) \geq 1 - \xi_i \\ \quad \xi_i \geq 0, (i = 1, 2, \cdots, m). \end{cases} \tag{16}$$

In order to solve this optimization problem, the dot product given by $\phi(x_i)^T\phi(x_j)$needs to be computed. However, it is difficult to calculate the dot product directly. Thus, this is usually obtained by computing the kernel function. The kernel $k(x_i, x_j)$ is given by $k(x_i, x_j) = \phi(x_i)^T\phi(x_j)$.There are four types kernel functions frequently used including linear, polynomial, radial basis function (RBF), and sigmoid kernels. As the most frequently used kernel function, RBF kernel is adopted here and it is expressed with Eq. 17:

$$k(x_i, x_j) = \exp\left(-\gamma\left\|x_i - x_j\right\|^2\right). \tag{17}$$

The parameter of γ greatly affects the number of support vector, which has a close relation with training time. Parameter γ also controls the amplitude of the Gaussian function which affects the generalization ability of SVM [24].

Thus, a suitable SVM model can be obtained according to the given samples data where parameters that the user has to specify are the kernel function, the value of C, and the value of γ. In this study, the values of C and γ are determined by a grid search method using cross-validation. The main idea about this method is that different parameter values are tested and the one with the best cross-validation accuracy is picked. This method is implemented in two steps. In the first step, a coarser grid is applied with an exponentially growing sequence of (C, γ) with $C = 2^{-5}, 2^{-3}, \cdots, 2^{7}, 2^{9}, \gamma = 2^{-9}, 2^{-7}\cdots, 2^{3}, 2^{5}$. After identifying the better region on the grid, the finer grid search on that region can be executed. The results are used to perform the final training process [25]. Then, the SVM model can be built by using the optimal parameters.

As discussed above, SVM basically is a binary classier. In order to deal with multi-classification problem, multiple binary classifiers are needed. It means that every sub-model

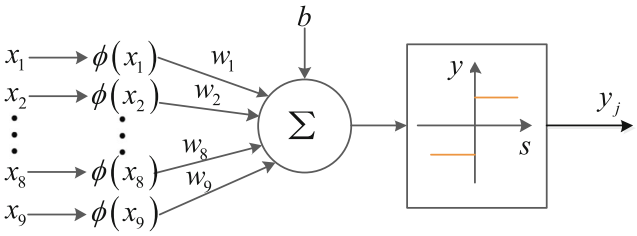

Fig. 9 The schematic diagram of SVM classification method

is designed according to the sample data of any two kinds of welding seam types. In this paper, the input of the SVM model is the feature vector of the structured-light image of the corresponding welding seam. The output of SVM model is the type number of the welding seam. The numbers 1, 2, 3, 4, 5, and 6 are used to represent six different welding seam types, respectively. Thus, C_6^2 sub-models need to be designed according to the samples data of six welding seam types. When classifying an unknown sample, we can get 15 classification results according to 15 sub-models. The welding seam type that occurs most frequently in classification results is chosen as the type of the welding seam.

5 Experiments and results

To verify the effectiveness of automatic recognition system of welding seam type, a series of experiments about six typical welding seam types were conducted. The experimental setup is shown in Fig. 10.

5.1 Welding seam type recognition based on SVM

The laser vision sensor was installed at the robot end link, and 50 different structured-light images of each welding seam type were captured. The parameters used in the image processing were set as follows: Δy = 50 pixel, $\alpha_1 = 1$, $\alpha_2 = 2$, $\alpha_3 = 1$, d_T = 3 pixel, and d_t = 2 pixel. Then, fivefold cross-validation method was used to find optimal parameters. In detail, the experiment data was divided into five parts, where four parts were used to model building and one part is used to model testing. By using the grid search method based on cross-validation, the optimal

Fig. 10 The experimental system

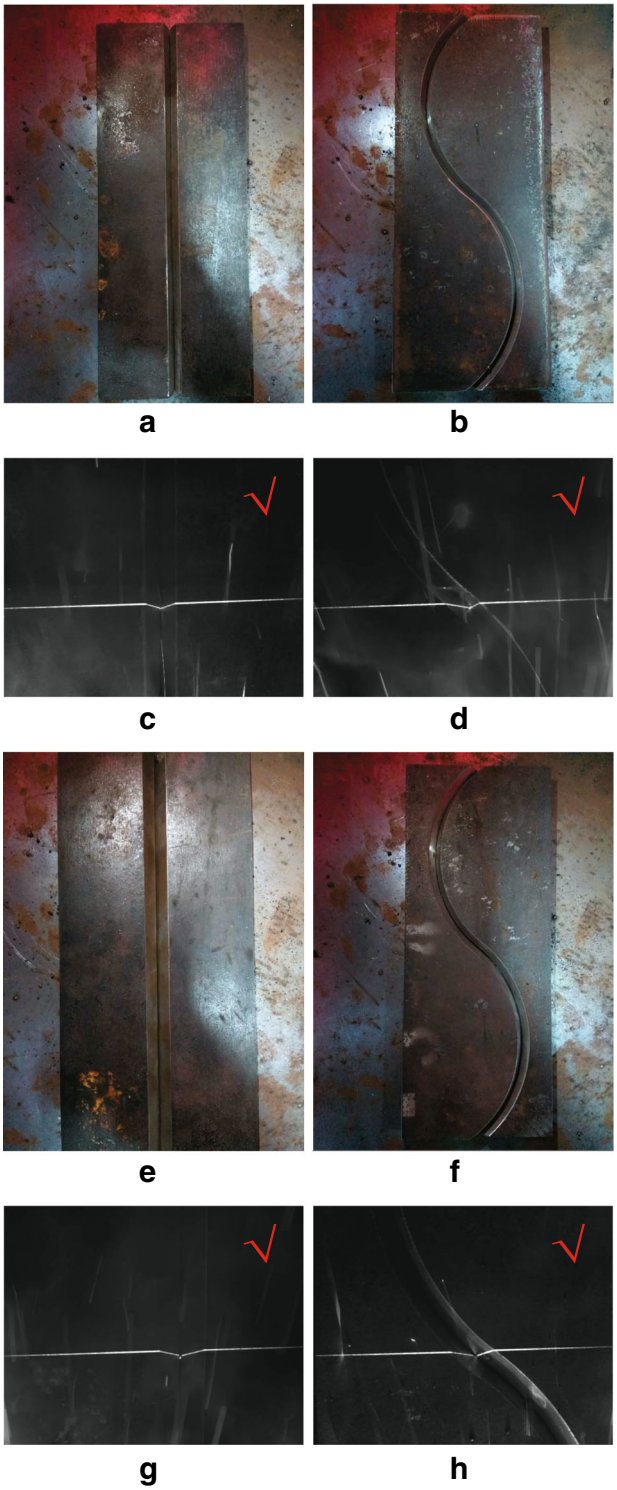

Fig. 11 Some testing samples of symmetric V groove. **a** The straight welding seam with small size of groove. **b** The curved welding seam with small size of groove. **c** The structured-light image of the straight welding seam with small size of groove. **d** The structured-light image of the curved welding seam with small size of groove. **e** The straight welding seam with big size of groove. **f** The curved welding seam with big size of groove. **g** The structured-light image of the straight welding seam with big size of groove. **h** The structured-light image of the curved welding seam with big size of groove

parameters C and γ of RBF were determined as $C = 128$ and $\gamma = 0.5$. Then, the SVM model was built by using the optimal parameters.

In order to verify effectiveness of welding seam type recognition system, workpieces with different sizes of grooves of straight welding seam and curved welding seam were tested. Taking symmetric V groove as an example, some structured-light images of different testing samples are shown in Fig. 11. Furthermore, in order to verify the robustness of the system, different types of noises were applied to images such as salt and pepper noise, gauss noise, and speckle noise. In this paper, the noise density of salt and pepper noise is 0.2. The mean and variance of gauss noise are 0 and 0.04, respectively. The mean and variance of speckle noise are 0 and 0.08 respectively. Taking symmetric V groove as an example, structured-light images with and without noises are shown in Fig. 12.

The results of the performance of the SVM model are presented in Table 1. It clearly shows that the proposed welding seam type recognition system based on SVM method is effective and robust. At the same time, with the computer that has the main frequency of 3.6 GHz and has the RAM of 8 GB, the processing time of welding seam type recognition based on the algorithm in [19] was 872.03 ms. However, with the same computation platform, the processing time of the proposed method in this paper was only 151.09 ms. Thus, the computation cost is reduced largely.

Table 1 Comparative performance of SVM and ANN in welding seam type recognition

Case	Case description	Accuracy of SVM (%)	Accuracy of ANN (%)
1	Without noise	97.33	94.0
2	Salt and pepper noise	97.33	94.0
3	Gauss noise	97.33	94.0
4	Speckle noise	97.33	93.33

5.2 Welding seam type recognition based on BPNN

To validate the proposed recognition system of welding seam type further, comparison experiments were conducted with the BP neural network (BPNN) method. A standard three-layer BPNN was used as a benchmark. There were nine nodes in the input layer $h_1 \sim h_9$, fifteen nodes in the hidden layer, and one node in the output layer. For the input layer, the input feature vector computation method was the same as the above-mentioned. For the hidden and output layers, the hidden nodes used the tansig transfer function and the output node used the purelin transfer function. The Levenberg-Marquardt method was used for training the BPNN, and fivefold cross validation method was used for testing. Similarly, structured-light images with and without

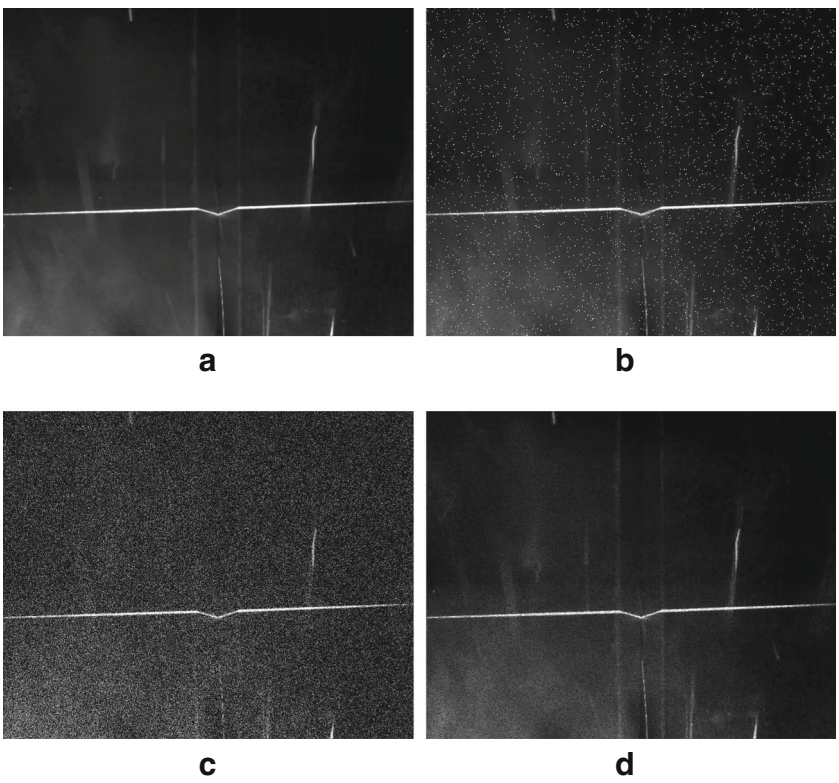

Fig. 12 Structured-light images of symmetric V groove. **a** The structured-light image without noises. **b** The structured-light image with salt and pepper noise. **c** The structured-light image with gauss noise. **d** The structured-light image with speckle noise

noises were used as samples to test effectiveness and robustness of BPNN model. The results of the performance of the BPNN models are also presented in Table 1. It shows that the SVM model's effectiveness and robustness for welding seam type recognition is better than that of BPNN because it adapts to the little sample problems and can avoid the local extreme.

6 Conclusions

An automatic recognition system of welding seam types based on SVM method is presented in this paper. Both input feature vector computation and model building methods are described in detail. The following conclusions are drawn:

1. Most of noises from arc lights and splashes can be filtered out by using a narrow band optical filter and "min operation," that is the prerequisite for welding seam type recognition.
2. The proposed feature vector computation method and SVM-based modeling method can distinguish different welding seam types effectively.
3. Experimental results show that the proposed system can achieve welding seam type recognition accurately even if there are some noises in the structured light image, and the computation cost can be reduced compared with previous methods.

In the future, we will combine the proposed welding seam type recognition system with the seam tracking system to realize automatic seam tracking of various welding seam types.

Acknowledgments This work was supported by the National Natural Science Foundation of China under Grant 61305024, 61273337, 61573358, and by the Foundation for Innovative Research Groups of the National Natural Science Foundation of China under Grant 61421004.

The authors would like to thank the anonymous referees for their valuable suggestions and comments.

References

1. Umeagukwu C, Maqueira B, Lambert R (1989) Robotic acoustic seam tracking: system development and application. IEEE Trans Indust Electron 36(3):338–348
2. Bae KY, Park JH (2006) A study on development of inductive sensor for automatic weld seam tracking. J Mater Process Technol 176(1):111–116
3. Mahajan A, Figueroa F (1997) Intelligent seam tracking using ultrasonic sensors for robotic welding. Robotica 15(03):275–281
4. Xu YL, Zhong JY, Ding MY, Chen HB, Chen SB (2013) The acquisition and processing of real-time information for height tracking of robotic GTAW process by arc sensor. Int J Adv Manuf Technol 65(5-8):1031–1043
5. Wang LK, Xu D, Tan M (2004) Robust detection for the weld seam shaped zigzag line. In: Proceedings of the IEEE International Conference on Robotics and Biomimetics, Shenyang, China, pp 721–726
6. Gu WP, Xiong ZY, Wan W (2013) Autonomous seam acquisition and tracking system for multi-pass welding based on vision sensor. Int J Adv Manuf Technol 69:451–460
7. Xu D, Wang LK, Tu ZG, Tan M (2005) Hybrid visual servoing control for robotic arc welding based on structured light vision. Acta Autom Sin 31(4):596–605
8. Kiddee P, Fang ZJ, Tan M (2016) An automated weld seam tracking system for thick plate using cross mark structured light. The International Journal of Advanced Manufacturing Technology pp 1–15
9. Xu YL, Fang G, Chen SB, Zou JJ, Ye Z (2014) Real-time image processing for vision-based weld seam tracking in robotic GMAW. Int J Adv Manuf Technol 73(9-12):1413–1425
10. Xu YL, Yu HW, Zhong JY, Lin T, Chen SB (2012) Real-time seam tracking control technology during welding robot GTAW process based on passive vision sensor. J Mater Process Technol 212(8):1654–1662
11. Gao XD, Na SJ (2005) Detection of weld position and seam tracking based on Kalman filtering of weld pool images. J Manuf Syst 24(1):1–12
12. Ge JG, Zhu ZQ, He DF, Chen LG (2005) A vision-based algorithm for seam detection in a PAW process for large-diameter stainless steel pipes. Int J Adv Manuf Technol 26(9-10):1006–1011
13. Xu D, Fang ZJ, Chen HY, Yan ZG, Tan M (2012) Compact visual control system for aligning and tracking narrow butt seams with CO2 gas-shielded arc welding. Int J Adv Manuf Technol 62(9-12):1157–1167
14. Guo B, Shi YH, Yu GQ, L B WK (2016) Weld deviation detection based on wide dynamic range vision sensor in MAG welding process. The International Journal of Advanced Manufacturing pp 1–14
15. Nele L, Sarno E, Keshari A (2013) An image acquisition system for real-time seam tracking. Int J Adv Manuf 69(9):2099–2110
16. L XQ, Zhang K, Wu YX (2016) The seam position detection and tracking for the mobile welding robot. The International Journal of Advanced Manufacturing Technology pp 1–10
17. Fang ZJ, Xu D, Tan M (2010) Visual seam tracking system for butt weld of thin plate. Int J Adv Manuf Technol 49(5-8):519–526
18. Qian BF, Liu NS, Liu MY, Lin HL (2007) Automatic recognition to the type of weld seam by visualsensor with structured light. J Nanchang Univ Eng Technol 29(4):368–370
19. Li Y, Xu D, Tan M (2006) Welding joints recognition based on Hausdorff distance. High Technol Lett 16(11):1129–1133
20. Li WH, Gao K, Wu J, Hu T, Wang JY (2014) SVM-based information fusion for weld deviation extraction and weld groove state identification in rotating arc narrow gap MAG welding. Int J Adv Manuf Technol 74(9-12):1355–1364
21. Vapnik VN (2000) The nature of statistical learning theory. SpringerVerlag, New York
22. Fang ZJ, Xu D, Tan M (2011) A vision-based self-tuning fuzzy controller for fillet weld seam tracking. IEEE/ASME Trans Mechatron 16(3):540–550
23. Vapnik VN (1999) An overview of statistical learning theory. IEEE Trans Neural Netw 10(5):988–999
24. Zhao C, Zhang H, Zhang X, Zhang R, Luan F, Liu M, Hu Z, Fan B (2006) Prediction of milk/plasma drug concentration (M/P) ratio using support vector machine (SVM) method. Pharm Res 23(1):41–48
25. Fei Z, Tiyip T (1074) A method of soil salinization information extraction with SVM classification based on ICA and texture features. Agric Sci Technol 15(7):1046–1049